Neuron
Article

Ca^{2+} Requirements for Cerebellar Long-Term Synaptic Depression: Role for a Postsynaptic Leaky Integrator

Keiko Tanaka,[1] Leonard Khiroug,[1,2] Fidel Santamaria,[1] Tomokazu Doi,[4] Hideaki Ogasawara,[4,5] Graham C.R. Ellis-Davies,[3] Mitsuo Kawato,[4] and George J. Augustine[1,*]
[1] Department of Neurobiology, Duke University Medical Center, Box 3209, Durham, NC 27710, USA
[2] Neuroscience Center, University of Helsinki, P.O. Box 65, Helsinki 00014, Finland
[3] Department of Pharmacology and Physiology, Drexel University College of Medicine, 245 North 15th Street, Philadelphia, PA 19102, USA
[4] Department of Computational Neurobiology, ATR Computational Neuroscience Laboratories, Kyoto 619-0288, Japan
[5] National Institute of Information and Communications Technology, Kyoto 619-0288, Japan
*Correspondence: georgea@neuro.duke.edu
DOI 10.1016/j.neuron.2007.05.014

SUMMARY

Photolysis of a caged Ca^{2+} compound was used to characterize the dependence of cerebellar long-term synaptic depression (LTD) on postsynaptic Ca^{2+} concentration ($[Ca^{2+}]_i$). Elevating $[Ca^{2+}]_i$ was sufficient to induce LTD without requiring any of the other signals produced by synaptic activity. A sigmoidal relationship between $[Ca^{2+}]_i$ and LTD indicated a highly cooperative triggering of LTD by Ca^{2+}. The duration of the rise in $[Ca^{2+}]_i$ influenced the apparent Ca^{2+} affinity of LTD, and this time-dependent behavior could be described by a leaky integrator process with a time constant of 0.6 s. A computational model, based on a positive-feedback cycle that includes protein kinase C and MAP kinase, was capable of simulating these properties of Ca^{2+}-triggered LTD. Disrupting this cycle experimentally also produced the predicted changes in the Ca^{2+} dependence of LTD. We conclude that LTD arises from a mechanism that integrates postsynaptic Ca^{2+} signals and that this integration may be produced by the positive-feedback cycle.

INTRODUCTION

Although many forms of long-lasting synaptic plasticity arise from the actions of Ca^{2+} within the postsynaptic neuron, in no case have the Ca^{2+} requirements for long-term plasticity been defined precisely (Augustine et al., 2003; Malenka and Bear, 2004). This question is of importance for understanding the mechanisms involved in synaptic plasticity, specifically how a postsynaptic Ca^{2+} signal is transduced into a long-lasting change in synaptic transmission. An understanding of the Ca^{2+} signals for long-term plasticity also is needed to explain how opposing forms of plasticity, such as long-term potentiation (LTP) and long-term depression (LTD), can both result from Ca^{2+} signals in the same postsynaptic neuron (Neveu and Zucker, 1996; Malenka and Bear, 2004; Coesmans et al., 2004; Nevian and Sakmann, 2006). This was first proposed to reflect a difference in postsynaptic Ca^{2+} requirements, with LTD induced by lower Ca^{2+} levels than LTP (Lisman, 1989; Artola and Singer, 1993), consistent with the Bienenstock-Cooper-Munro (BCM) rule of synaptic plasticity (Bienenstock et al., 1982). However, it is now thought that LTP and LTD result from different temporal patterns of $[Ca^{2+}]_i$ elevation (Yang et al., 1999) and/or different requirements for other signals generated by synaptic activity (Nevian and Sakmann, 2006).

Here we have examined the Ca^{2+} requirements for cerebellar LTD. This form of long-term synaptic plasticity arises when excitatory parallel fiber (PF) and climbing fiber (CF) inputs of Purkinje cells are activated concurrently (Linden, 1994; Ito, 2001). Many lines of evidence indicate that LTD arises from a transient rise in $[Ca^{2+}]_i$ in the postsynaptic Purkinje cell (Sakurai, 1990; Linden et al., 1991; Crépel and Jaillard, 1991; Konnerth et al., 1992; Shibuki and Okada, 1992; Kasono and Hirano, 1994; Lev-Ram et al., 1997; Miyata et al., 2000; Wang et al., 2000a). However the precise magnitude and duration of the Ca^{2+} signals required for LTD induction are not yet clear and may even follow a reversed BCM rule (Coesmans et al., 2004). To define these fundamental characteristics of LTD, we have used local uncaging to precisely control the amount and duration of Ca^{2+} elevation. With this approach, we found that the magnitude of LTD is determined by the level of $[Ca^{2+}]_i$, with LTD being triggered by Ca^{2+} in a highly cooperative manner. Further, the level of $[Ca^{2+}]_i$ required to induce LTD is dynamically regulated according to the duration of $[Ca^{2+}]_i$ elevation, indicating leaky integrator behavior. These properties are important for explaining how LTD is selectively induced by specific

patterns of synaptic activity. A computational model based on a positive-feedback signal transduction cycle (Kuroda et al., 2001) is capable of reproducing these emergent properties of LTD, suggesting that such interactions between signal transduction molecules underlie the triggering of LTD by postsynaptic Ca^{2+}.

RESULTS

DMNPE-4 Photolysis Locally Elevates $[Ca^{2+}]_i$

The goal of our experiments was to raise postsynaptic $[Ca^{2+}]_i$ and observe the resulting changes in PF synaptic transmission. $[Ca^{2+}]_i$ was elevated by using UV light to photolyze the caged Ca^{2+} compound, DMNPE-4 (Ellis-Davies, 1998). Upon photolysis, this compound undergoes a large drop in Ca^{2+} affinity that yields a rise in free $[Ca^{2+}]_i$ (Ellis-Davies and Barsotti, 2006). DMNPE-4 (10 mM) was dialyzed into voltage-clamped Purkinje cells for at least 30 min to allow time for dendritic diffusion. In our initial paradigm, DMNPE-4 was uncaged with brief (5 ms duration) UV light pulses, and the resultant rises in free $[Ca^{2+}]_i$ were monitored with the high-affinity indicator dye, Oregon Green 488 BAPTA-1 (K_d of 0.17 μM). The DMNPE-4 was photolyzed with a spot of UV light 5–10 μm in diameter (Wang and Augustine, 1995). When this light spot was focused on a distal region of a Purkinje cell, over fine dendrites, a localized rise in $[Ca^{2+}]_i$ was produced (Figure 1A). Three lines of evidence indicate that this increase in the fluorescence of the Ca^{2+} indicator dye arose specifically from light-induced release of Ca^{2+} from photolyzed DMNPE-4. First, including the Ca^{2+} chelator, BAPTA, in the intracellular solution along with the DMNPE-4 prevented the light-induced signal (data not shown), indicating that it was a genuine rise in $[Ca^{2+}]_i$. Second, UV illumination of Purkinje cells that were not dialyzed with DMNPE-4 did not cause any changes in $[Ca^{2+}]_i$. Third, UV illumination also had no effect on cell input resistance or holding current. This indicates that the rise in $[Ca^{2+}]_i$ was genuine and not caused by phototoxicity.

The rise in $[Ca^{2+}]_i$ produced by uncaging DMNPE-4 was transient (Figure 1B). $[Ca^{2+}]_i$ was maximal immediately after UV exposure (within the 33 ms image acquisition time) and then rapidly returned to the resting level. The time constant for decay of the rise in $[Ca^{2+}]_i$ was 90 ± 17 ms (n = 3). This rapid decline in $[Ca^{2+}]_i$ presumably was due to removal of Ca^{2+} from the site of photolysis, such as by the action of Ca^{2+} pumps on plasma membrane and endoplasmic reticulum, although sequestration by Ca^{2+}-binding proteins and Ca^{2+}-free DMNPE-4 may also contribute (Fierro et al., 1998; Maeda et al., 1999; Schmidt et al., 2003; Sepúlveda et al., 2004). We next quantified the size of this region of elevated $[Ca^{2+}]_i$ by measuring $[Ca^{2+}]_i$ along the length of a dendrite (Figure 1C). The spatial range of $[Ca^{2+}]_i$ elevation could be described by a Gaussian function with a peak at the center of uncaging spot and a half-width of 7.9 ± 2.0 μm (n = 4). This range was similar to the size of the UV light spot, consistent with a previous report that Ca^{2+} does not spread far from the site of uncaging in Purkinje cell dendrites (Santamaria et al., 2006).

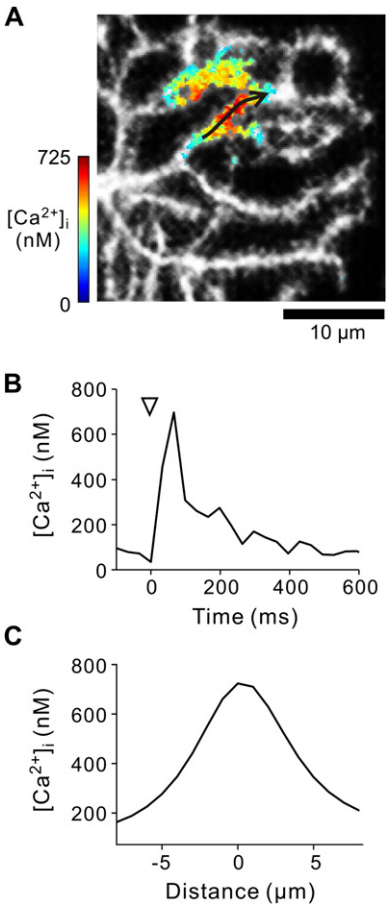

Figure 1. Temporal and Spatial Dynamics of $[Ca^{2+}]_i$ Changes Produced by Uncaging DMNPE-4 in Purkinje Cells

(A) Fluorescence image of a Purkinje cell dendrite. Pseudocolor overlay indicates changes in $[Ca^{2+}]_i$ following DMNPE-4 uncaging.

(B) Time course of $[Ca^{2+}]_i$ signal in (A). $[Ca^{2+}]_i$ changes were integrated over a length of 3 μm centered at the uncaging spot. ∇ indicates time of uncaging.

(C) Spatial profile of $[Ca^{2+}]_i$ along the dendrite in (A) at t = 66 ms; 0 indicates center of the uncaging spot, and numbers correspond to the direction of arrow in (A).

When the brief light pulses were repeatedly applied at 1 Hz, to emulate the trains of synaptic activity traditionally used to induce LTD (Crépel and Jaillard, 1991; Konnerth et al., 1992; Karachot et al., 1994; Chen and Thompson, 1995), transient increases in $[Ca^{2+}]_i$ occurred in response to each pulse (see Figure 2A and Figure S1A in the Supplemental Data available with this article online). In addition, there was a slow increase in baseline $[Ca^{2+}]_i$ that accumulated during the train. The increase in $[Ca^{2+}]_i$ remained very localized, spreading only 53% ± 18% (n = 3) more at the fifth pulse than at the first pulse and spreading no further during the remaining 25 pulses in the train, again presumably due to Ca^{2+} removal mechanisms.

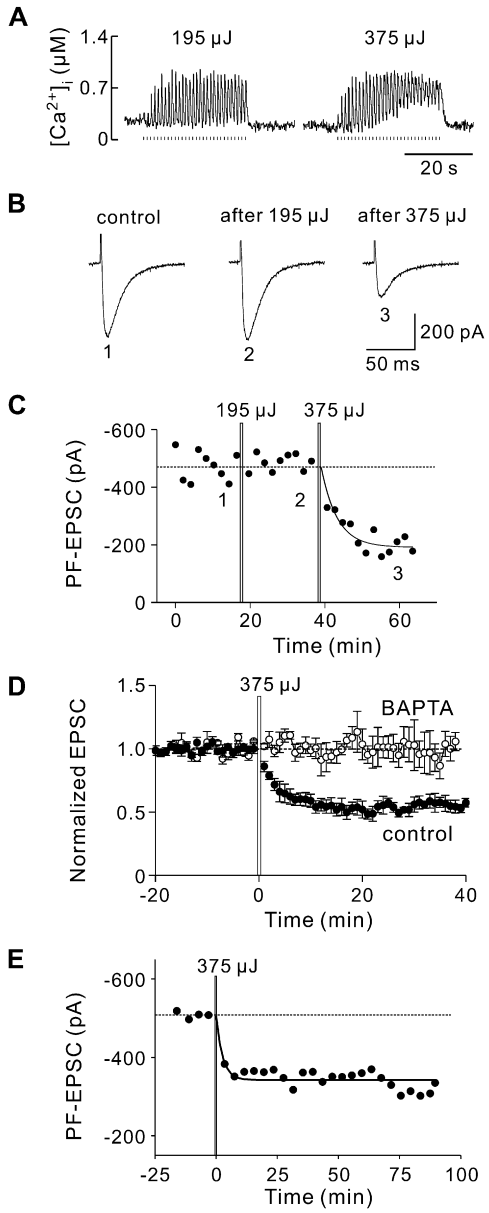

Figure 2. Induction of LTD by Trains of $[Ca^{2+}]_i$ Increases

(A) Time course of $[Ca^{2+}]_i$ changes produced in a Purkinje cell by two trains of UV light pulses. Light energies are indicated above the traces, and timing of the light pulses is indicated below.

(B) PF-EPSCs recorded before and after each of the light trains shown in (A). Numbers indicate times (in [C]) when each trace was recorded.

(C) Time course of changes in PF-EPSC amplitude resulting from the light trains shown in (A).

(D) LTD induced by uncaging DMNPE-4 (10 mM; filled circles) is blocked by including the Ca^{2+} chelator, BAPTA (20 mM), in the intracellular solution (open circles). PF-EPSC amplitudes are normalized to the mean pretrain level for each condition, and error bars indicate SEM.

(E) Persistence of Ca^{2+}-induced LTD for 90 min after Ca^{2+} uncaging.

Elevated $[Ca^{2+}]_i$ Is Sufficient to Induce LTD

It has been postulated that the ultimate signal for LTD is a local rise in $[Ca^{2+}]_i$, produced by IP3-mediated release of Ca^{2+} from endoplasmic reticulum within spines of PF synapses (Berridge, 1993; Finch and Augustine, 1998; Miyata et al., 2000; Wang et al., 2000a). To determine whether such a rise in $[Ca^{2+}]_i$ is sufficient to induce LTD, we elevated $[Ca^{2+}]_i$ at the same sites where an extracellular electrode was placed to stimulate PF axons and evoke excitatory postsynaptic currents (PF-EPSCs). A representative experiment is shown in Figures 2A–2C. In this experiment, a 1 Hz train of low-intensity light pulses for 30 s (5 ms duration, 6.5 μJ per pulse, 195 μJ total) was used to elevate $[Ca^{2+}]_i$ (Figure 2A, left). During the time that $[Ca^{2+}]_i$ was elevated, PF stimulation was halted to prevent generation of other signals produced by PF activity. Resumption of PF stimulation indicated that this rise in $[Ca^{2+}]_i$ did not change PF-EPSC amplitude (Figures 2B and 2C). Higher-intensity light pulses (12.5 μJ per pulse, 375 μJ total) elevated $[Ca^{2+}]_i$ faster and to higher levels, particularly during the baseline between pulses (Figure 2A, right). Such elevation of $[Ca^{2+}]_i$ produced an LTD-like depression of the amplitude of PF-EPSCs (Figures 2B and 2C). Similar results were obtained in eight independent experiments, with uncaging Ca^{2+} producing on average a 52% ± 4% reduction in PF-EPSC amplitude that developed with a time constant of 6.5 ± 1.1 min.

To determine whether the depression of PF-EPSCs was due directly to Ca^{2+}, we repeated the experiments while chelating intracellular Ca^{2+} by including BAPTA (20 mM) in the intracellular solution. In the presence of BAPTA, there was no measurable decline in PF-EPSCs for more than 30 min after illuminating three different Purkinje cells with UV light (Figure 2D, open symbols, 375 μJ total). However, when BAPTA was not added to the intracellular solution, the same illumination paradigm caused PF-EPSCs to be depressed to 46% ± 1% (n = 5) of their initial amplitudes (Figure 2D, filled symbols). This result demonstrates that the depression of PF synaptic transmission is caused by Ca^{2+} rather than by UV illumination or by the other by-products of the photolysis reaction, such as free DMNPE-4 cage.

Further experiments, described in the Supplemental Data, establish that the Ca^{2+}-induced depression of PF synaptic transmission shares many properties with the LTD that results from pairing PF synaptic activity with Purkinje cell depolarization. First, like the Ca^{2+} signals resulting from CF activity, uncaged Ca^{2+} can be paired with PF activity to depress PF-EPSCs (Figure S1). Second, the Ca^{2+}-induced depression of PF-EPSCs requires clathrin-dependent internalization of postsynaptic AMPA receptors (Figure S2A), as does LTD (Wang and Linden, 2000). Third, Ca^{2+}-induced depression of PF transmission and synaptically induced LTD can occlude each other (Figure S2B), indicating that these two long-lasting forms of synaptic modification share common signal transduction pathways. Because of these similarities, we conclude that Ca^{2+} is sufficient to cause LTD in the absence of PF or CF activity. By varying the distance between the sites of Ca^{2+} uncaging and PF stimulation, we also could conclude that Ca^{2+}-dependent LTD was limited to sites where $[Ca^{2+}]_i$ was elevated (Figure S3).

LTD apparently consists of early and late phases, with the early phase resulting from posttranslational regulation of AMPA receptor trafficking (Wang and Linden, 2000; Matsuda et al., 2000; Chung et al., 2003) and the late phase caused by changes in gene expression (Linden, 1996). Studies with protein synthesis inhibitors indicate that the early phase develops over a few minutes, while the late phase begins ~60 min after inducing LTD in cultured Purkinje cells (Linden, 1996) as well as in cerebellar slices (K.T. and G.J.A., unpublished data). The LTD induced by uncaged Ca^{2+} persisted for as long as the recording lasted, with no evidence of recovery even 80–100 min after elevating $[Ca^{2+}]_i$ (Figure 2E). On average, PF-EPSCs were depressed by 45% ± 5% (n = 3) at 80–100 min after elevating $[Ca^{2+}]_i$. Thus, uncaging Ca^{2+} locally in PF dendrites apparently is sufficient to produce both the early and late phases of LTD.

Ca^{2+} Requirements for LTD Induction

Our results indicate that raising $[Ca^{2+}]_i$ to a sufficient level, via photolysis of DMNPE-4, can induce LTD without requiring any additional signals that may be generated by the activity of PF or CF synapses. This greatly simplifies analysis of the signaling events involved in LTD. Photolysis of DMNPE-4 also simplifies analysis of the amount of intracellular Ca^{2+} required to induce LTD by avoiding the complex spatial dynamics of $[Ca^{2+}]_i$ changes associated with entry of Ca^{2+} into the Purkinje cell cytoplasm via membrane ion channels (Ross and Werman, 1987; Konnerth et al., 1992; Eilers et al., 1996). However, photolysis by trains of brief light pulses still produced temporally complex changes in $[Ca^{2+}]_i$ (e.g., Figure 2A and Figure S1A). Therefore, to quantify the relationship between $[Ca^{2+}]_i$ and LTD, we simplified the kinetics of $[Ca^{2+}]_i$ elevation by using a single, prolonged pulse of very dim UV light and varied the amount of $[Ca^{2+}]_i$ by changing the peak intensity of this pulse.

The prolonged light pulses elevated $[Ca^{2+}]_i$ monotonically and were capable of eliciting LTD. The experiment shown in Figures 3A and 3B illustrates a case where the UV light pulses were 1 s in duration. In this example, raising $[Ca^{2+}]_i$ to 0.5 μM (150 μJ) or to 1 μM (250 μJ) failed to induce LTD, as indicated by a lack of change in PF-EPSC amplitude. However, elevating $[Ca^{2+}]_i$ to a higher level, with a 400 μJ pulse that raised $[Ca^{2+}]_i$ to 1.4 μM, elicited LTD. In contrast, elevating $[Ca^{2+}]_i$ to 0.8 μM (200 μJ) twice was insufficient to induce LTD (Figure S4). Thus, there appears to be a sharp threshold level of $[Ca^{2+}]_i$ required to induce LTD.

By using 1 s duration light pulses to vary $[Ca^{2+}]_i$ in 17 different experiments, it was possible to define the quantitative relationship between the peak value of $[Ca^{2+}]_i$ and the amount of LTD (Figure 3C). In these experiments, $[Ca^{2+}]_i$ sometimes was raised to several μM, so we used a low-affinity indicator, Oregon Green 488 BAPTA-6F (K_d = 3.4 μM), to measure $[Ca^{2+}]_i$. The relationship between $[Ca^{2+}]_i$ and LTD was sigmoidal, with no LTD produced at $[Ca^{2+}]_i$ levels of 1 μM or lower and full LTD elicited at

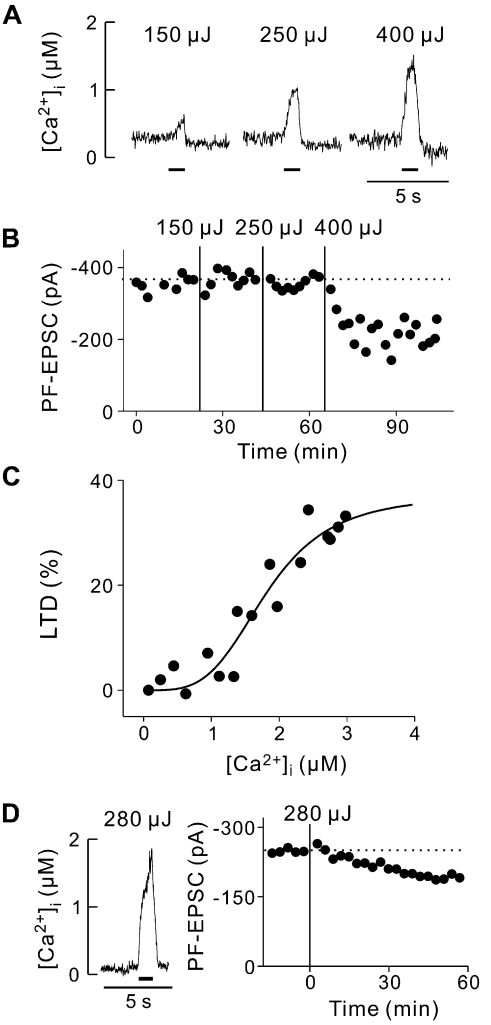

Figure 3. Ca^{2+} Requirements for LTD

(A) Time course of $[Ca^{2+}]_i$ increases evoked in a Purkinje cell by three UV pulses (horizontal bars; 1 s duration) of different intensities.

(B) Time course of changes in PF-EPSC amplitude resulting from the $[Ca^{2+}]_i$ increases shown in (A).

(C) Relationship between peak $[Ca^{2+}]_i$ changes and amount of LTD. Curve indicates fit of the Hill equation.

(D) Intermediate rise in $[Ca^{2+}]_i$ (left) caused an intermediate amount of LTD (right).

$[Ca^{2+}]_i$ of 2.5 μM or greater. Intermediate amounts of LTD sometimes were observed at intermediate $[Ca^{2+}]_i$ (Figure 3D). The relationship shown in Figure 3C could be described by the Hill equation:

$$LTD = LTD_{max}\left[\frac{[Ca^{2+}]_i^n}{K_{Ca}^n + [Ca^{2+}]_i^n}\right]$$

where the Hill coefficient (n) was 3.8 ± 1.3, indicating a highly cooperative triggering of LTD by Ca^{2+}. The calculated maximal depression of PF-EPSCs (LTD_{max}) was 37.2% ± 7.9% and the concentration of Ca^{2+} required for half-maximal LTD (K_{Ca}) was 1.8 ± 0.3 μM.

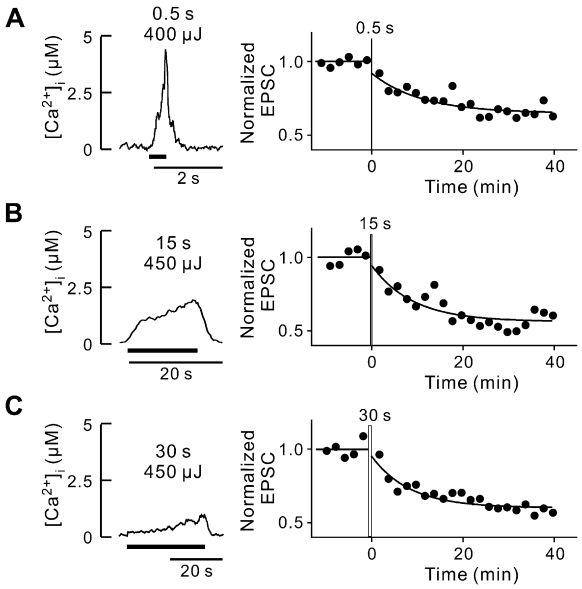

Figure 4. Examples of LTD Induced by Rises in $[Ca^{2+}]_i$ of Different Durations

Rises in $[Ca^{2+}]_i$ (left) and changes in PF-EPSCs (right) induced by 0.5 s (A), 15 s (B), or 30 s (C) long light pulses. LTD developed with time constants of 11 (A), 9 (B), and 8.4 min (C). Light energy is indicated above each plot.

Dynamic Ca^{2+} Requirements for LTD

Induction of LTD depends upon the duration of synaptic activity (Karachot et al., 1994). Because this relationship may arise from the properties of Ca^{2+} triggering of LTD, we next determined how LTD depends upon the amount of time that $[Ca^{2+}]_i$ is elevated. This was done by varying the duration of the UV light pulses from 0.5 to 30 s, yielding ramp-like rises in $[Ca^{2+}]_i$ of variable duration (Figure 4, left). Sufficient elevation of $[Ca^{2+}]_i$ was capable of producing LTD at each duration (Figure 4, right). The relationship between $[Ca^{2+}]_i$ and the amount of LTD was sigmoidal for each duration and could be described by the Hill equation (Figure 5A). Prolonged elevation of $[Ca^{2+}]_i$ caused a leftward shift in this relationship. This shift arose because the K_{Ca} value was lower with longer durations of light (Figure 5B). Thus, the duration of $[Ca^{2+}]_i$ elevation influences the Ca^{2+} requirements for LTD induction. In contrast, the maximal amount of LTD was independent of the duration of $[Ca^{2+}]_i$ elevation (Figure 5C). The Hill coefficient was also comparable for all durations and was ~5 (Figure 5D). These results indicate that the Ca^{2+} sensitivity of LTD is a dynamic process that depends on how long $[Ca^{2+}]_i$ is elevated in the postsynaptic Purkinje cell.

The time-dependent increase in the apparent Ca^{2+} sensitivity of LTD shown in Figure 5 suggests that the LTD induction mechanism can integrate Ca^{2+} signals over time. To evaluate the integrative properties of LTD induction, we examined the relationship between LTD and the time integral of $[Ca^{2+}]_i$ for different durations of elevated $[Ca^{2+}]_i$.

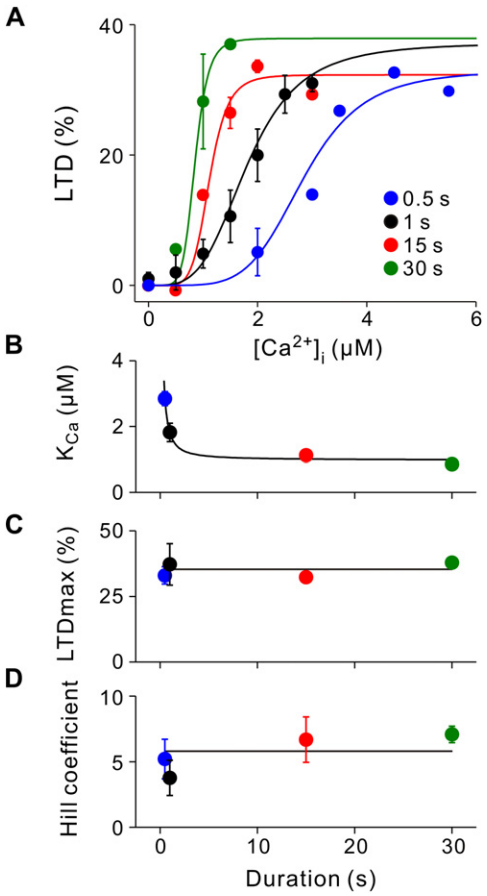

Figure 5. Ca^{2+} Dependence of LTD Depends on Duration of $[Ca^{2+}]_i$ Rise

(A) Relationship between peak $[Ca^{2+}]_i$ and LTD for different durations of $[Ca^{2+}]_i$ elevation. Smooth curves indicate fits of the Hill equation; note that the data are plotted on linear coordinates. 1 s data are from same experiments shown in Figure 3C. Error bars indicate SEM. Total number of experiments ranged from 5 to 17 for different durations; each point represents 1 to 3 experiments.

(B–D) Influence of duration of $[Ca^{2+}]_i$ elevation on K_{Ca} values (B), maximum amount of LTD (C), and Hill coefficient (D). Error bars indicate two standard deviations of parameter estimates.

These relationships were sigmoidal, saturating at high levels of integrated Ca^{2+} (Figure 6A). The curves obtained with 0.5 and 1 s duration pulses virtually superimposed, indicating precise integration of Ca^{2+} over this time frame. However, at longer durations the relationships diverged and shifted to the right (red and green points in Figure 6A). As a result, the half-maximal amount of integrated $[Ca^{2+}]_i$ required for LTD ($K_{Ca\text{-}integ}$; Figure 6B) increased over time, a time dependence that was opposite that observed for the relationship between LTD and peak $[Ca^{2+}]_i$ (Figure 5B). The maximal amount of LTD and the Hill coefficient remained virtually independent of the duration of $[Ca^{2+}]_i$ elevation (Figures 6C and 6D). We therefore conclude that the amount of Ca^{2+} within the dendrites of Purkinje cells is integrated during LTD, but this integration

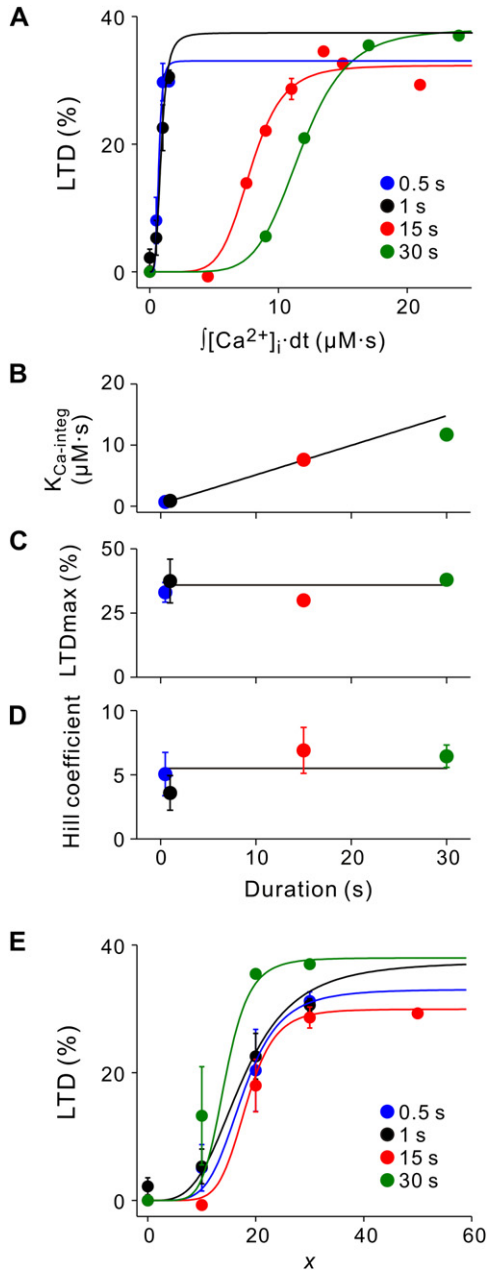

Figure 6. Integration of Ca^{2+} during LTD

(A) Relationship between integrated amount of Ca^{2+} and LTD; data from same experiments shown in Figure 5. Error bars indicate SEM.

(B–D) Influence of duration of $[Ca^{2+}]_i$ elevation on $K_{Ca\text{-}integ}$ (B), maximum amount of LTD (C), and Hill coefficient (D). Error bars indicate two standard deviations of parameter estimates.

(E) Data from Figure 5A transformed by calculating x from Equation 2.

mechanism is imperfect and becomes less efficient during prolonged elevation of $[Ca^{2+}]_i$.

Our results indicate that LTD induction can be considered as a "leaky integrator" process, similar to the "leaky integrate and fire" concept often used in models of neuronal electrical signaling (Knight, 1972; Fohlmeister et al., 1977). For the case of Ca^{2+} triggering of LTD, such a leaky integrator can be described mathematically as

$$\tau \frac{dx}{dt} = -x + a\left[Ca^{2+}\right]_i(t) \quad (1)$$

where τ is the time constant of the integration, x is the amount of a downstream signal that transduces Ca^{2+} into LTD, and a is a scaling factor representing the efficiency of the integrator in converting Ca^{2+} into x. As detailed in the Supplemental Data, when $[Ca^{2+}]_i$ is elevated in a ramp-like fashion, as in our experiments (Figures 3A and 4), the solution of Equation 1 is

$$x(t) = ak\,\tau \exp\left(-\frac{t}{\tau}\right) + ak(t-\tau) \quad (2)$$

where k is the rate of increasing $[Ca^{2+}]_i$, i.e., peak $[Ca^{2+}]_i$ divided by the light pulse duration, t. We used this function to fit the dependence of K_{Ca} on light pulse duration; a good fit was obtained (smooth curve in Figure 5B) when τ was 0.56 s and a was 18.7%/μM. With these values, Equation 2 also provided a reasonable description of the dependence of $K_{Ca\text{-}integ}$ on light pulse duration (line in Figure 6B). The ability of Equation 2 to describe the time dependence of K_{Ca} and $K_{Ca\text{-}integ}$ indicates that Ca^{2+} induction of LTD can be described as a leaky integrator process.

To further test the leaky integrator proposal, we used Equation 2 to transform the relationship between peak $[Ca^{2+}]_i$ and amount of LTD (Figure 5A). When peak $[Ca^{2+}]_i$ at the end of the UV pulse was converted into the corresponding value of x, the curves obtained at all light pulse durations superimposed (Figure 6E). This loss of duration dependence indicates that the dynamic properties observed experimentally arise from the leaky integrator behavior, supporting the idea that LTD results from Ca^{2+} activating signaling processes that behave as a leaky integrator with a time constant of ~0.6 s.

Computational Simulation of Ca^{2+} Requirements for LTD

To consider the mechanisms underlying the leaky integrator properties of LTD, we employed the computational model of LTD signaling, which was developed by Kuroda et al. (2001) from the signal transduction schemes first described by Bhalla and Iyengar (1999). Although this model (Figure 7A) was not originally designed to simulate the results of experiments that directly manipulated $[Ca^{2+}]_i$, in fact with only four minor modifications (see Supplemental Data) this model reproduced the major features of our experimental data very well. For example, the model predicted the threshold behavior of LTD and also reproduced the experimental observation that the relationship between LTD and peak $[Ca^{2+}]_i$ shifts leftward as $[Ca^{2+}]_i$ is elevated for longer times (Figure 7B).

However, the model predicted that LTD was essentially an all-or-none function of $[Ca^{2+}]_i$, abruptly going from nearly no LTD to maximal LTD over a very narrow range

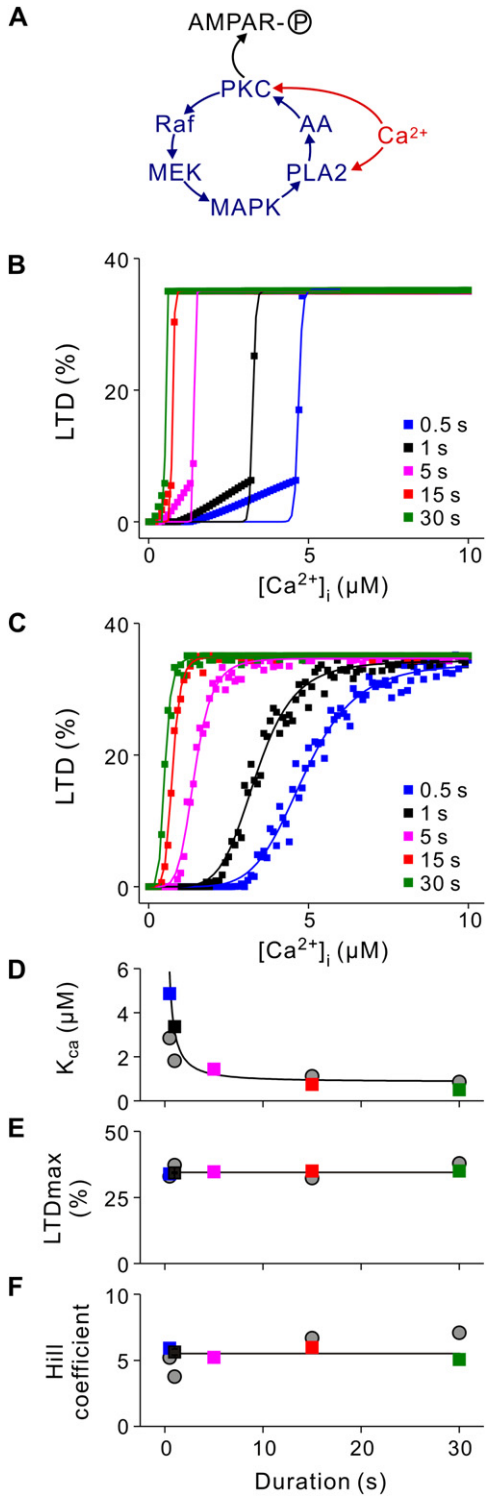

Figure 7. A Computational Model of LTD

(A) Diagram of the signaling components proposed to be activated by Ca^{2+} during LTD. $[Ca^{2+}]_i$ elevation results in AMPA receptor phosphorylation by activating PKC, both directly and indirectly via a positive-feedback loop. Molecules involved in the positive-feedback loop are shown in blue.

of $[Ca^{2+}]_i$. Because such bistable behavior was not observed in our experimental measurements, we next refined the model by taking into account the experimental conditions. In particular, we transformed the model predictions (as described in Supplemental Data) by considering the spatial gradients in $[Ca^{2+}]_i$ that occurred during local uncaging (see Figures 1A and 1C) and the noise associated with experimental measurements of $[Ca^{2+}]_i$ and PF-EPSCs. After including these two factors, the model very accurately simulated experimental measurements of the relationship between peak $[Ca^{2+}]_i$ and LTD (Figure 7C). Fits of the Hill equation to the simulation results indicated that K_{Ca} was sensitive to the duration of $[Ca^{2+}]_i$ elevation (Figure 7D), while the maximum amount of LTD (Figure 7E) and the Hill coefficient (Figure 7F) were duration independent. In all of these regards, the simulations closely paralleled the experimental measurements shown in Figure 5. Further, the values of K_{Ca}, maximum amount of LTD, and Hill coefficient determined for the simulation results were very similar to those measured experimentally, as can be seen in Figures 7D–7F by comparing simulation values (colored symbols) to the experimental measurements (gray symbols). Thus, the model emulated the dynamic properties of LTD induction by Ca^{2+}.

To further compare the model predictions to the experimental measurements, we also plotted the predicted relationship between integrated $[Ca^{2+}]_i$ and the amount of LTD. Consistent with the leaky integrator properties observed in the experiments, the model reproduced the rightward shift caused by prolonging the duration of $[Ca^{2+}]_i$ elevation (Figure 8A). The $K_{Ca\text{-}integ}$ value also increased with longer durations (Figure 8B), while the maximal amount of LTD and Hill coefficient were duration independent (Figures 8C and 8D). The predicted values for $K_{Ca\text{-}integ}$, maximum amount of LTD, and Hill coefficient also were very similar to those measured experimentally (compare colored and gray symbols in Figures 8B–8D), although the $K_{Ca\text{-}integ}$ values for longer durations were slightly smaller than those observed in the experimental measurements. As was the case for the experimental data, the mathematical description of a leaky integrator (Equation 2) could be fit to the simulation data (lines in Figures 7D and 8B). The best-fitting value of τ was 1.52 s, and a was 20.4%/μM, which are in the same range as the values obtained from the experimental measurements. As was the case for the experimental measurements, the influence of duration was greatly reduced when Equation 2 was used to transform the data in Figure 7C by

(B) Simulated relationships between peak $[Ca^{2+}]_i$ and LTD for different durations of $[Ca^{2+}]_i$ elevation.

(C) Results of simulation, after taking into account nonuniform spatial distribution of $[Ca^{2+}]_i$ and noise in experimental measurements.

(D–F) K_{Ca} value (D), maximum amount of LTD (E), and Hill coefficient (F) determined from fits of the Hill equation to the relationships shown in (C). For comparison, experimental data shown in Figures 5B–5D are also plotted as gray circles. Smooth curve in (D) is derived from Equation 2.

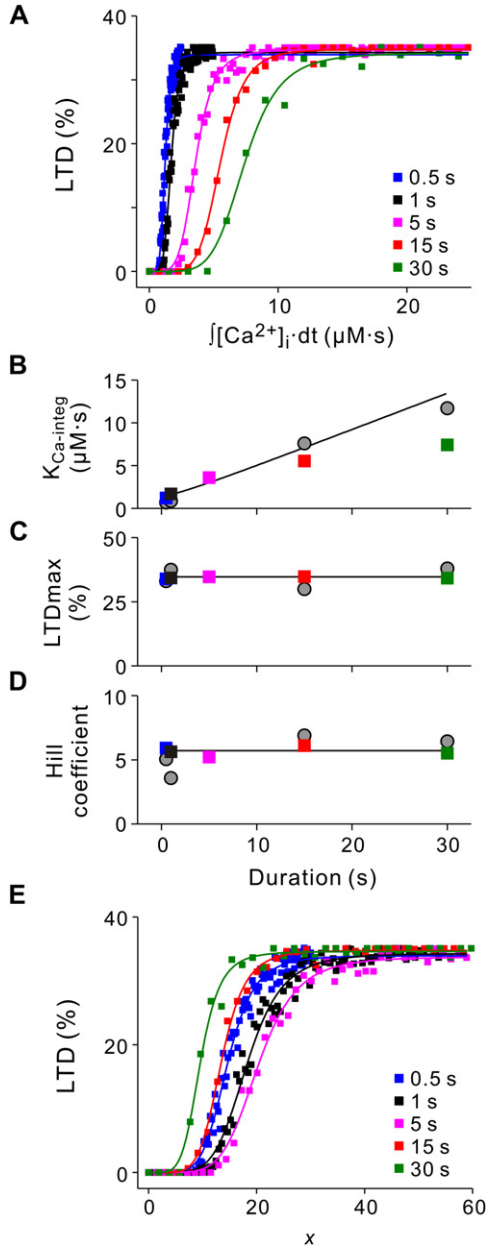

Figure 8. Integration of Ca^{2+} in the Computational Model

(A) Relationship between integrated $[Ca^{2+}]_i$ and LTD predicted by the computational simulation.

(B–D) Values for $K_{Ca\text{-}integ}$ (B), maximum amount of LTD (C), and Hill coefficient (D) derived from fits of the Hill equation to the simulation data in (A). For comparison, experimental data shown in Figures 6B–6D are also plotted as gray circles.

(E) Transformation of data of Figure 7C by using Equation 2 to calculate *x*.

converting peak $[Ca^{2+}]_i$ into *x* (Figure 8E). We therefore conclude that the simulation was capable of reproducing many significant features of Ca^{2+} triggering of LTD, including threshold behavior, cooperativity, saturation, and leaky integration.

We next used the predictive power of the model to address the origins of these properties of LTD. The main feature of the model is the positive-feedback loop that includes protein kinases and several other signal transduction molecules (Figure 7A). To determine whether this positive-feedback mechanism underlies the Ca^{2+}-dependent triggering of LTD, we disrupted the feedback loop computationally by preventing activation of protein kinase C (PKC) by arachidonic acid (AA), while leaving unchanged the activity of all other enzymes. The model predicted that the relationships between LTD and both peak $[Ca^{2+}]_i$ (Figure 9A and Figure S8A) and integrated $[Ca^{2+}]_i$ (Figure 9B) will change in the absence of the positive-feedback loop.

To quantify the effects of loop disruption, we focused on the relationship between integrated $[Ca^{2+}]_i$ and LTD (Figures 9C–9E). A similar analysis for the relationship between peak $[Ca^{2+}]_i$ and LTD is provided in the Supplemental Data (Figures S8B–S8D). Loss of the positive-feedback loop increased K_{Ca} values, specifically at intermediate durations of $[Ca^{2+}]_i$ elevation, and increased $K_{Ca\text{-}integ}$ values at longer durations of $[Ca^{2+}]_i$ elevation (Figure 9C). Disrupting the positive-feedback loop also was predicted to affect the maximum of LTD, which was predicted to vary according to the duration of $[Ca^{2+}]_i$ elevation (Figure 9D). This indicates a loss of the all-or-none character of LTD and is also predicted by the model before taking into account the experimental conditions (Figure S8E). Further, loss of the loop greatly reduced the Hill coefficient for Ca^{2+} triggering of LTD (Figure 9E). Fits of Equation 2 to these data (assuming a fixed threshold for LTD even though LTD was no longer predicted to be all-or-none) yielded estimates of 0.32 s for τ and 5.0%/μM for *a*, Thus, loss of the positive-feedback loop reduces the strength of integration (smaller *a*) and increases leakiness (faster τ). In summary, the model predicted that disrupting the positive-feedback loop will affect Ca^{2+} induction of LTD, in particular causing a loss of the all-or-none character of LTD, reducing the cooperative triggering of LTD by Ca^{2+}, and lowering the effectiveness of the leaky integrator.

To test these predictions, we returned to experimental measurements and asked whether disruption of the proposed positive-feedback loop affects the Ca^{2+} dependence of LTD induction. For this purpose, we treated slices with OBAA, a potent and selective inhibitor of phospholipase A2 (PLA2; Köhler et al., 1992; Bastianetto et al., 2000) that prevents LTD induction in response to synaptic activity (Reynolds and Hartell, 2001). We considered two extreme durations of $[Ca^{2+}]_i$ elevation: 1 and 30 s. In the presence of OBAA (5 μM), 1 s long rises in $[Ca^{2+}]_i$ had very little ability to trigger LTD (Figures 9F and 9G and Figure S8F). Even when peak $[Ca^{2+}]_i$ was high (3–4 μM), the magnitude of LTD was only half of the maximum value of LTD observed in the absence of OBAA. With 30 s light pulses, high $[Ca^{2+}]_i$ (2–3 μM) produced LTD that was similar in magnitude to what was observed in control conditions (Figures 9F and 9G and Figure S8F). Analysis of

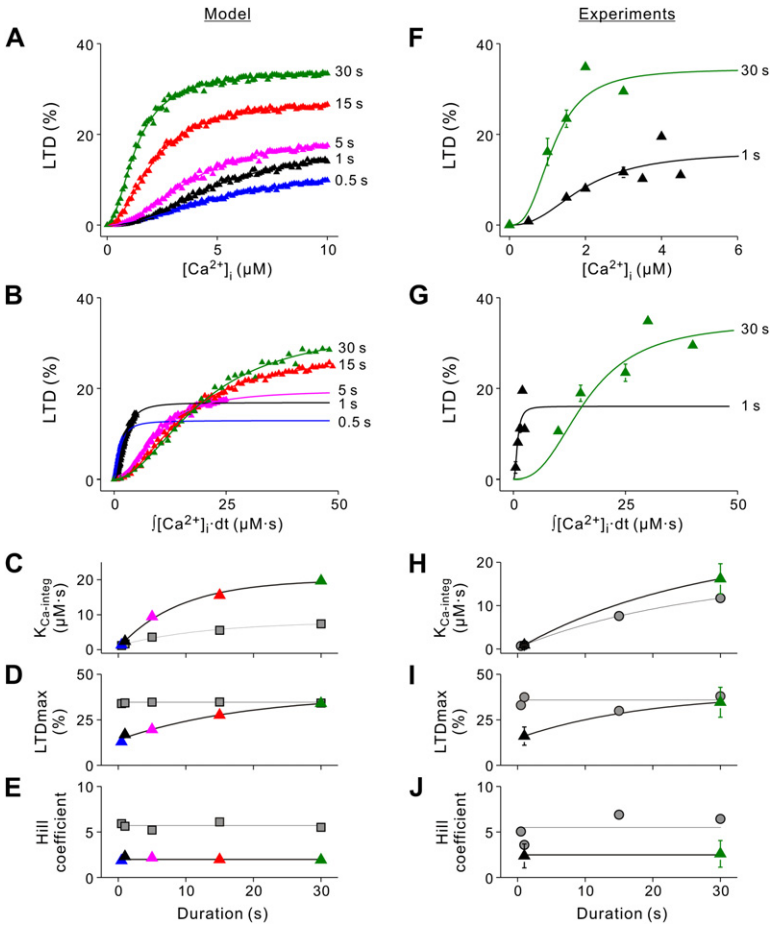

Figure 9. Effects of Disrupting the Postulated Positive-Feedback Loop

Results of the computational simulation (A–E) are compared to experimental results (F–J).

(A) Relationship between peak $[Ca^{2+}]_i$ and LTD predicted by simulation in the absence of activation of PKC by AA. Simulation data were corrected for the effects of nonuniform distribution of $[Ca^{2+}]_i$ and noise, as in Figure 7.

(B) Relationship between integrated $[Ca^{2+}]_i$ and LTD predicted by simulation in the absence of activation of PKC by AA.

(C–E) Values of $K_{Ca\text{-}integ}$ (C), maximum amount of LTD (D), and Hill coefficient (E) obtained from Hill equation fits of the data shown in (B). For comparison, control data obtained by computational simulation with positive-feedback loop intact (Figures 8B–8D) are also plotted as gray squares.

(F) Relationship between peak $[Ca^{2+}]_i$ and LTD measured experimentally in the presence of a PLA2 inhibitor. Points represent means of binned results from individual experiments; black symbols indicate results for 1 s pulses (n = 11) and green indicates 30 s pulses (n = 9).

(G) Experimentally measured relationship between integrated $[Ca^{2+}]_i$ and LTD, derived from the experiments shown in (F). Error bars indicate SEM.

(H–J) Values of $K_{Ca\text{-}ingteg}$ (H), maximum amount of LTD (I), and Hill coefficient (J) derived from Hill equation fits to the experimental data in (G). For comparison, gray circles replot control experimental data (Figures 6B–6D). Error bars indicate two standard deviations of parameter estimates.

these relationships indicated that application of OBAA somewhat increased the $K_{Ca\text{-}integ}$ value at 30 s (Figure 9H) and greatly reduced the Hill coefficient for both durations (Figure 9J). Further, OBAA significantly ($p < 0.05$) reduced the maximum amount of LTD elicited by elevating $[Ca^{2+}]_i$ for 1 s but not for 30 s (Figure 9I). In all these regards, the experimental data closely resembled the predictions of the computational model. The close correspondence between computational and experimental results suggests that the steep, cooperative triggering of LTD by Ca^{2+}—attributed to a leaky integrator—arises, at least in part, from the positive-feedback mechanism incorporated into the model.

DISCUSSION

We have used photolysis of caged Ca^{2+} (Ellis-Davies, 2003) to quantify the ability of postsynaptic Ca^{2+} to trigger LTD at the PF-Purkinje cell synapse. Elevation of Ca^{2+} to peak levels of a few micromolar or less was sufficient to induce LTD without requiring any of the additional signals that normally are associated with activity at PF or CF synapses. Ca^{2+} triggering of LTD was dynamic: the duration of Ca^{2+} elevation influenced the Ca^{2+} sensitivity of LTD, with higher sensitivity to peak $[Ca^{2+}]_i$ and lower sensitivity to integrated $[Ca^{2+}]_i$ at longer duration. This dynamic behavior could be described quantitatively as a leaky integrator process with a time constant of ~0.6 s. These properties of Ca^{2+} triggering of LTD could be reproduced by a computational model based on a positive-feedback relationship between several protein kinases. Disrupting this loop was predicted to affect Ca^{2+} triggering of LTD, and experimental perturbation of this feedback loop produced the predicted effects on Ca^{2+} induction of LTD. This work illustrates new properties of Ca^{2+} triggering of a form of long-term synaptic plasticity and implicates the positive-feedback loop in Ca^{2+} action during LTD.

Calcium Requirements for LTD

Cerebellar LTD has long been known to depend on elevation of Ca^{2+} concentration within the postsynaptic Purkinje cell. The earliest evidence for this came from experiments showing that postsynaptic introduction of the Ca^{2+} chelators EGTA (Sakurai, 1990; Shibuki and Okada, 1992) and BAPTA (Konnerth et al., 1992) blocks LTD and that stimuli which induce LTD also elevate $[Ca^{2+}]_i$ in Purkinje cells (Konnerth et al., 1992). Moreover, several treatments that elevate postsynaptic $[Ca^{2+}]_i$—such as depolarization (Linden et al., 1991; Crépel and Jaillard, 1991; Konnerth et al., 1992), strong PF activity (Hartell, 1996; Eilers

et al., 1997), and photolysis of caged Ca^{2+} compounds (Kasono and Hirano, 1994; Lev-Ram et al., 1997)—can be paired with PF activity or glutamate application to induce LTD. Our results have extended these observations by showing that elevated postsynaptic Ca^{2+} alone can suffice to induce LTD as long as $[Ca^{2+}]_i$ exceeds a threshold level. Photolysis of caged Ca^{2+} compounds did not induce LTD in previous studies (Kasono and Hirano, 1994; Lev-Ram et al., 1997); although $[Ca^{2+}]_i$ was not determined in these studies, we presume that $[Ca^{2+}]_i$ was below the threshold for inducing LTD in these experiments. The presence of a threshold can also explain why CF activity alone is insufficient to induce LTD (Ito and Kano, 1982; Chen and Thompson, 1995): activation of CF synapses elevates $[Ca^{2+}]_i$ by a few hundred nM for ~0.5 s (Konnerth et al., 1992; Eilers et al., 1995; Wang et al., 2000a), which is below the threshold for inducing LTD during such brief rises in $[Ca^{2+}]_i$ (Figure 5A).

During trains of brief pulses of light, we often observed a sustained rise in basal $[Ca^{2+}]_i$ (Figure 2A and Figure S1A). These sustained rises in $[Ca^{2+}]_i$ appeared to be more effective in triggering LTD than were the larger transient rises in $[Ca^{2+}]_i$. For example, while the peak levels of $[Ca^{2+}]_i$ are very similar for the two trains of $[Ca^{2+}]_i$ responses shown in Figure 2A, only the right response, which also had a sustained rise in $[Ca^{2+}]_i$, was capable of inducing LTD (Figures 2B and 2C). Such behavior emerges from the leaky integrator property of LTD, which makes LTD more sensitive to prolonged elevation of $[Ca^{2+}]_i$ (Figure 5A). The leaky integrator property of LTD may also account for the observation that LTD induction requires prolonged trains of paired PF and CF activity (Karachot et al., 1994). Pairing of single PF and CF stimuli induces only transient $[Ca^{2+}]_i$ increases, lasting for ~0.2 s (Wang et al., 2000a; Doi et al., 2005; Hernjak et al., 2005). Because such responses cannot induce LTD, it is likely that only repeated pairing of PF and CF activity causes a sustained increase in $[Ca^{2+}]_i$ that can be integrated to cause LTD. Paradoxically, it has been reported that prolonging the duration of paired synaptic activity, from 300 to 500 s, causes a reduction in LTD expression (Karachot et al., 1994). Such behavior could be explained by the leakiness of the integrator, which causes the effectiveness of Ca^{2+} to decline over time.

It has been proposed that cerebellar LTD results from a local, suprathreshold Ca^{2+} signal produced when IP3 receptors are synergistically activated by subthreshold IP3 signals, produced by active PFs, and subthreshold Ca^{2+} signals produced by CF activity (Berridge, 1993; Finch and Augustine, 1998; Miyata et al., 2000; Wang et al., 2000a; Doi et al., 2005; Hernjak et al., 2005). Two of our results provide additional support for this model. First, we found that LTD was induced by pairing a subthreshold amount of $[Ca^{2+}]_i$ with PF stimulation (Figure S1). Second, we found that a rise in $[Ca^{2+}]_i$ alone is sufficient to cause LTD as long as $[Ca^{2+}]_i$ exceeds a threshold. Thus, our results are consistent with the idea that IP3 receptors serve as a coincidence detector for LTD.

Our definition of the $[Ca^{2+}]_i$ requirements for cerebellar LTD is one of the only efforts to quantify the relationship between postsynaptic $[Ca^{2+}]_i$ and induction of long-lasting synaptic plasticity. Coesmans et al. (2004) have proposed that cerebellar LTD is induced by relatively high (but unspecified) levels of $[Ca^{2+}]_i$ and that LTP is induced by lower $[Ca^{2+}]_i$ levels. While we could confirm that micromolar amounts of postsynaptic Ca^{2+} could induce LTD, in fact we did not observe LTP in response to elevation of $[Ca^{2+}]_i$ to lower levels (e.g., Figures 3C and 5A). This discrepancy could arise because LTP requires not only an increase in $[Ca^{2+}]_i$ but also another signal that is produced by synaptic activity, such as NO (Lev-Ram et al., 2002; Namiki et al., 2005). Our observation that elevating $[Ca^{2+}]_i$ in Purkinje cells to ~0.9 μM for 30 s yielded LTD (Figure 5A) is in line with a report that elevating $[Ca^{2+}]_i$ in hippocampal CA1 pyramidal cells to ~0.8 μM for 60 s caused LTD (Yang et al., 1999). Thus, in terms of the BCM rule, cerebellar LTD can be triggered by the same "low" Ca^{2+} signal that produces hippocampal LTD. This similarity is remarkable, given that these two forms of LTD are known to differ substantially in their signal transduction mechanisms (Malenka and Bear, 2004). These differences in mechanism could explain why hippocampal LTD apparently does not exhibit a well-defined $[Ca^{2+}]_i$ threshold (Neveu and Zucker, 1996). Differences in signal transduction mechanisms presumably also account for our observation that cerebellar LTD could also be induced by relatively large and brief rises in $[Ca^{2+}]_i$ (e.g., ~5 μM for 0.5 s), even though brief elevation of $[Ca^{2+}]_i$ in hippocampal neurons, to levels on the order of 10 μM, induces LTP rather than LTD (Yang et al., 1999).

Because we uncaged Ca^{2+} in highly localized (5–10 μm diameter) regions of distal dendrites of Purkinje cells, our results provide information about the spatial range of signaling during LTD. First, we found that the late phase of LTD can be elicited by local elevation of $[Ca^{2+}]_i$ in dendrites (Figure 2E). Given that the late phase of LTD apparently requires changes in nuclear gene expression (Linden, 1996), this suggests that localized rises in dendritic $[Ca^{2+}]_i$ are capable of producing other, mobile signal(s) that can reach the nucleus to regulate gene expression. The nature of such dendrite-to-nucleus signaling is not yet clear (Deisseroth et al., 1998). Second, while the early component of LTD is known to spread ~50 μm from active PF synapses to inactive ones (Wang et al., 2000b; Reynolds and Hartell, 2000), we found that Ca^{2+}-induced LTD does not spread beyond the site of Ca^{2+} uncaging (Figure S3). CF activity and/or depolarization elevate $[Ca^{2+}]_i$ throughout the Purkinje cell (Ross and Werman, 1987; Konnerth et al., 1992; Miyakawa et al., 1992). This subthreshold rise in Ca^{2+} can be viewed as being permissive for the spread of early LTD, although some other signal produced by PF activity—such as NO (Reynolds and Hartell, 2001; Ogasawara et al., 2007) or glutamate (Marcaggi et al., 2003)—must mediate and spatially limit the spread of LTD (Hartell, 2002).

The relationships between postsynaptic $[Ca^{2+}]_i$ and LTD induction (Figures 5A and 6A) were sigmoidal with Hill coefficients of ~5, indicating that LTD is cooperatively triggered by Ca^{2+}. Our computational model was capable of producing very similar values of Hill coefficient, suggesting that the signaling reactions included in the model are responsible for the cooperative behavior. The model predicted that the Hill coefficient should be reduced by loss of the positive-feedback loop (Figure 9E), and this was observed experimentally when we disrupted the loop (Figure 9J). These results indicate that the loop is involved in the cooperative triggering of LTD and are consistent with previous proposals that such positive-feedback mechanisms are a source of biochemical cooperativity (Ferrell and Machleder, 1998). In the absence of the positive-feedback loop, the Hill coefficient was still ~2. This residual cooperativity may arise from direct activation of PKC; this enzyme is known to be cooperatively activated by 2 Ca^{2+} (Sutton and Sprang, 1998; Verdaguer et al., 1999). Thus, it appears that the highly cooperative triggering of LTD by Ca^{2+} arises from the concerted actions of Ca^{2+} on the positive-feedback loop and on PKC directly.

All-or-None Behavior of LTD

The sigmoidal Ca^{2+} dependence of LTD confers threshold behavior, in the sense that small rises in $[Ca^{2+}]_i$ are insufficient to trigger LTD. Our computational model predicted such behavior and, in fact, predicted even more extreme, bistable behavior at the level of individual synapses (Figure 7B). Thus, the model predicts that LTD has all-or-none properties, as has been proposed for hippocampal LTP (Petersen et al., 1998). Our analysis indicated that spatial nonuniformities in $[Ca^{2+}]_i$ and noise largely blurs this behavior, so that LTD appeared to be a graded function of $[Ca^{2+}]_i$ in our experimental measurements. Experimental analysis of LTD at the level of individual synapses (Casado et al., 2002) will be required to evaluate all-or-none behavior critically. However, all-or-none behavior was evident in our experimental observation that the maximum amount of LTD produced by saturating $[Ca^{2+}]_i$ was constant for all durations of $[Ca^{2+}]_i$ elevation (Figures 5C and 6C), even though the amount of $[Ca^{2+}]_i$ required for LTD varied. The model predicts that the all-or-none behavior of LTD results from the positive-feedback loop, so that disrupting this loop will cause the maximum amount of LTD to depend upon how long $[Ca^{2+}]_i$ is elevated (Figure 9D). This prediction was confirmed by our experimental measurements in the presence of a PLA2 inhibitor (Figure 9I), providing further support for the idea that LTD is an all-or-none process and that this is due to the positive-feedback loop.

Dynamic Ca^{2+} Triggering of LTD by a Leaky Integrator

We have discovered that the amount of $[Ca^{2+}]_i$ required to initiate LTD is a time-dependent variable. To our knowledge, such behavior has not been described previously for cerebellar LTD, even though a dynamic threshold is a central tenet of the BCM theory of cortical plasticity (Bienenstock et al., 1982) and has been proposed as a requirement for encoding the history of synaptic activity (Bear, 1995). Mathematically, the dynamics of Ca^{2+} triggering of LTD could be described as a leaky integrator with a time constant of ~0.6 s. We view LTD in the same way that neuronal electrical signaling is described as a "leaky integrate and fire" mechanism, with the "firing" being an all-or-none activation of the signal transduction network that yields LTD.

Although our computational model of LTD signaling consists of a single chemical compartment, the model was able to reproduce the leaky integrator behavior accurately (Figures 7D and 8B). Further, integration was greatly reduced in the absence of the positive-feedback loop (Figures S8B and S8G), demonstrating that this loop is part of the integration mechanism. Integration was still present at a low level in the absence of this loop, indicating that integration does not depend entirely upon the loop. A simple hypothesis is that integration arises both from the kinetics of direct activation of PKC by Ca^{2+} (Oancea and Meyer, 1998), as well as from the ability of the positive-feedback loop to prolong activation of PKC (Kuroda et al., 2001). The "leakiness" indicates the presence of reactions that oppose Ca^{2+} triggering of LTD. Loss of the positive-feedback loop amplified the leakiness (Figures 9C and 9H), indicating that this loop counteracts the leakiness. Leakiness could arise from a phosphatase reversing the effect of PKC (Shenolikar, 1986). One specific candidate for the leak is protein phosphatase 2A, which is constitutively active in Purkinje cells and limits LTD induction (Launey et al., 2004).

The key feature of our computational model, as first proposed by Kuroda et al. (2001), is the positive-feedback signal transduction loop (Bhalla and Iyengar, 1999). This model is consistent with previous demonstrations that LTD requires several enzymes proposed to participate in the loop, such as PKC, MAP kinase, and PLA2 (Ito, 2001). The concordance between our experiments and the emergent predictions of this model provides an experimental indication that the positive-feedback loop is important for LTD; several more experimental tests in progress provide stronger support for this model (K.T. and G.J.A., 2006, Soc. Neurosci., abstract). Although loss of the positive-feedback loop altered the relationship between $[Ca^{2+}]_i$ and LTD induction, LTD could still be induced without this loop. This residual LTD, which was graded in amplitude and less sensitive to Ca^{2+}, probably arises because Ca^{2+} can still activate PKC directly in the absence of the feedback loop.

Conclusions

We have found that a rise in postsynaptic Ca^{2+} concentration is sufficient to induce cerebellar LTD. Because of the cooperative triggering of LTD by Ca^{2+}, LTD is induced only when $[Ca^{2+}]_i$ exceeds a certain level. The amount of Ca^{2+} required for LTD is relatively low, in the micromolar range, but depends upon the amount of time that Ca^{2+}

concentration is elevated. This time dependence arises from the leaky integrator properties of the LTD induction process. These characteristics of Ca^{2+} activation can explain many of the features of LTD induction following synaptic activity and are predicted by a computational model that postulates a central role for a positive-feedback loop of signal transduction enzymes.

EXPERIMENTAL PROCEDURES

Patch-Clamp Recordings

Whole-cell patch-clamp recordings were made from Purkinje cells as described previously (Miyata et al., 2000; Wang et al., 2000b). Sagittal slices (200–250 μm thick) were prepared from cerebella of 14- to 21-day-old rats or mice. Consistent with a previous study (Miyata et al., 2000), the time course and spatial distribution of $[Ca^{2+}]_i$ elevation after uncaging Ca^{2+} and the properties of Ca^{2+}-induced LTD were similar in slices from rats and mice. Slices were bathed in extracellular solution containing (in mM) 119 NaCl, 2.5 KCl, 1.3 Mg_2SO_4, 2.5 $CaCl_2$, 1.0 NaH_2PO_4, 26.2 $NaHCO_3$, 10 glucose, and 0.01 bicuculline methiodide (all from Sigma). A PLA2 inhibitor, OBAA (5 μM; Tocris), was added into the extracellular solution as indicated. Patch electrodes (2–4 MΩ) were filled with a pipette solutions containing (in mM) 130 potassium gluconate, 2 NaCl, 4 $MgCl_2$, 4 Na_2-ATP, 0.4 Na-GTP, 20 HEPES (pH 7.3), 0.25 Ca^{2+} indicator (Oregon Green 488 BAPTA-1 or 6F; Molecular Probes), 10 caged Ca^{2+} compound (DMNPE-4; synthesized by G. Ellis-Davies), and 6 $CaCl_2$ (pH adjusted to 7.2 with KOH). In some experiments, BAPTA (20 mM; Molecular Probes) or AP2 and AP2 ΔDLL peptides (1.6 mM; Morgan et al., 2000) were included in the intracellular solution. EPSCs were evoked in Purkinje cells (clamped at –60 mV) by activating parallel fibers with a glass stimulating electrode (5–10 μm tip diameter) filled with extracellular solution and placed on the surface of the molecular layer. Details of our procedures for stimulating parallel fibers can be found in Wang et al. (2000b). PF-EPSCs were acquired and analyzed using LTP software (W.W. Anderson, University of Bristol, UK) (Anderson and Collingridge, 2001). Data were accepted if series resistance changed less than 20%, input resistance was between 100 to 150 MΩ, holding current changed less than 5%, and $[Ca^{2+}]_i$ returned to baseline following photolysis of caged Ca^{2+}. Statistical comparisons between experimental groups were performed with the Student's t test (Figure S2A) or a Z test (Figure 9I). LTD was calculated as the change in PF-EPSC amplitude averaged over 10 min period ~40 min after $[Ca^{2+}]_i$ elevation, or in the last 10 min in cases where the recording did not last for 40 min.

Optical Techniques

Procedures described previously (Miyata et al., 2000) were used to examine the response of Purkinje cells to uncaged Ca^{2+}. In brief, cells were dialyzed with a solution containing a fluorescent indicator and DMNPE-4, and the set-up described in Wang and Augustine (1995) was used to uncage Ca^{2+}. UV light (351–364 nm) from an argon ion laser (Coherent model 305) was delivered to the slice, via an optical fiber and an Olympus 40× water-immersion objective, to make a light spot with a half-width of 5–10 μm that was focused on the primary or secondary dendrites of a Purkinje cell. The duration of UV exposure was controlled by an electronic shutter. When UV light pulses of 1 s or longer in duration were delivered, neutral density filters were used to reduce light intensity by 90%. UV energy was measured at the optical plane, so that reported values reflect the amount of light delivered to the slice.

Oregon Green fluorescence was imaged using a high-speed confocal microscope (Noran Odyssey XL), and $[Ca^{2+}]_i$ values were calculated from the ratio of increased fluorescence to basal fluorescence ($R = \Delta F/F_0$) using the following equation (Swandulla et al., 1991):

$$\left[Ca^{2+}\right]_i = \left(F_d \times K_d \times (R+1) - K_d \times F_{min}\right)/\left(F_{max} - F_d \times (R+1)\right)$$

$$F_d = \left(F_{max} \times \left[Ca^{2+}\right]_{rest} + K_d \times F_{min}\right)/\left(K_d + \left[Ca^{2+}\right]_{rest}\right)$$

where K_d is the Ca^{2+} dissociation constant of the indicator and F_{min} and F_{max} were the minimum and maximum amounts of fluorescence emission in the absence and presence of Ca^{2+}, respectively. Resting $[Ca^{2+}]_i$ ($[Ca^{2+}]_{rest}$) was calculated as 72 nM (Augustine et al., 1991). In experiments with long light pulses (0.5–30 s), some bleaching occurred (e.g., Figure 3A) and was corrected for by separately measuring the rate of bleaching of Oregon Green 488 BAPTA-6F in acrylamide gel. Because $[Ca^{2+}]_i$ increased in a ramp-like manner during the time that Ca^{2+} was elevated (Figures 3A and 4), the integrated amount of Ca^{2+} was calculated by multiplying peak $[Ca^{2+}]_i$ by pulse duration and then dividing by 2. Statistical analysis was performed using Origin 7.0 (Microcal). Averaged data are presented as mean ± SEM.

Computational Simulation

To simulate the relationship between Ca^{2+} and LTD, we used the mathematical model of signal transduction pathways for cerebellar LTD described by Kuroda et al. (2001). A detailed description of our implementation of this model is described in the Supplemental Data (Figure S6).

Supplemental Data

The Supplemental Data for this article can be found online at http://www.neuron.org/cgi/content/full/54/5/787/DC1/.

ACKNOWLEDGMENTS

We thank Ken Berglund and Ryohei Yasuda for reading our manuscript. This work was supported by HFSP grant RGP0074/2003; NIH grants NS-34045, GM-65473, and GM-53395; a Uehara Memorial Foundation research grant; and a postdoctoral fellowship from the Japan Society for the Promotion of Science.

Received: December 15, 2006
Revised: March 30, 2007
Accepted: May 16, 2007
Published: June 6, 2007

REFERENCES

Anderson, W.W., and Collingridge, G.L. (2001). The LTP program: a data acquisition program for on-line analysis of long-term potentiation and other synaptic events. J. Neurosci. Methods *108*, 71–83.

Artola, A., and Singer, W. (1993). Long-term depression of excitatory synaptic transmission and its relationship to long-term potentiation. Trends Neurosci. *16*, 480–487.

Augustine, G.J., Adler, E.M., and Charlton, M.P. (1991). The calcium signal for transmitter secretion from presynaptic nerve terminals. Ann. N Y Acad. Sci. *635*, 365–381.

Augustine, G.J., Santamaria, F., and Tanaka, K. (2003). Local calcium signaling in neurons. Neuron *40*, 331–346.

Bastianetto, S., Zheng, W.H., and Quirion, R. (2000). The *Ginkgo biloba* extract (EGb 761) protects and rescues hippocampal cells against nitric oxide-induced toxicity: involvement of its flavonoid constituents and protein kinase C. J. Neurochem. *74*, 2268–2277.

Bear, M.F. (1995). Mechanism for a sliding synaptic modification threshold. Neuron *15*, 1–4.

Berridge, M.J. (1993). Cell signalling. A tale of two messengers. Nature *365*, 388–389.

Bhalla, U.S., and Iyengar, R. (1999). Emergent properties of networks of biological signaling pathways. Science *283*, 381–387.

Bienenstock, E.L., Cooper, L.N., and Munro, P.W. (1982). Theory for the development of neuron selectivity: orientation specificity and binocular interaction in visual cortex. J. Neurosci. *2*, 32–48.

Casado, M., Isope, P., and Ascher, P. (2002). Involvement of presynaptic N-methyl-D-aspartate receptors in cerebellar long-term depression. Neuron *33*, 123–130.

Chen, C., and Thompson, R.F. (1995). Temporal specificity of long-term depression in parallel fiber–Purkinje synapses in rat cerebellar slice. Learn. Mem. *2*, 185–198.

Chung, H.J., Steinberg, J.P., Huganir, R.L., and Linden, D.J. (2003). Requirement of AMPA receptor GluR2 phosphorylation for cerebellar long-term depression. Science *300*, 1751–1755.

Coesmans, M., Weber, J.T., De Zeeuw, C.I., and Hansel, C. (2004). Bidirectional parallel fiber plasticity in the cerebellum under climbing fiber control. Neuron *44*, 691–700.

Crépel, F., and Jaillard, D. (1991). Pairing of pre- and postsynaptic activities in cerebellar Purkinje cells induces long-term changes in synaptic efficacy in vitro. J. Physiol. *432*, 123–141.

Deisseroth, K., Heist, E.K., and Tsien, R.W. (1998). Translocation of calmodulin to the nucleus supports CREB phosphorylation in hippocampal neurons. Nature *392*, 198–202.

Doi, T., Kuroda, S., Michikawa, T., and Kawato, M. (2005). Inositol 1,4,5-trisphosphate-dependent Ca^{2+} threshold dynamics detect spike timing in cerebellar Purkinje cells. J. Neurosci. *25*, 950–961.

Eilers, J., Callewaert, G., Armstrong, C., and Konnerth, A. (1995). Calcium signaling in a narrow somatic submembrane shell during synaptic activity in cerebellar Purkinje neurons. Proc. Natl. Acad. Sci. USA *92*, 10272–10276.

Eilers, J., Plant, T., and Konnerth, A. (1996). Localized calcium signalling and neuronal integration in cerebellar Purkinje neurones. Cell Calcium *20*, 215–226.

Eilers, J., Takechi, H., Finch, E.A., Augustine, G.J., and Konnerth, A. (1997). Local dendritic Ca^{2+} signaling induces cerebellar long-term depression. Learn. Mem. *4*, 159–168.

Ellis-Davies, G.C.R. (1998). Synthesis of photosensitive EGTA derivatives. Tetrahedron Lett. *39*, 953–956.

Ellis-Davies, G.C.R. (2003). Development and application of caged calcium. Methods Enzymol. *360*, 226–238.

Ellis-Davies, G.C.R., and Barsotti, R.J. (2006). Tuning caged calcium: photolabile analogues of EGTA with improved optical and chelation properties. Cell Calcium *39*, 75–83.

Ferrell, J.E., Jr., and Machleder, E.M. (1998). The biochemical basis of an all-or-none cell fate switch in Xenopus oocytes. Science *280*, 895–898.

Fierro, L., DiPolo, R., and Llano, I. (1998). Intracellular calcium clearance in Purkinje cell somata from rat cerebellar slices. J. Physiol. *510*, 499–512.

Finch, E.A., and Augustine, G.J. (1998). Local calcium signalling by inositol-1,4,5-trisphosphate in Purkinje cell dendrites. Nature *396*, 753–756.

Fohlmeister, J.F., Poppele, R.E., and Purple, R.L. (1977). Repetitive firing: a quantitative study of feedback in model encoders. J. Gen. Physiol. *69*, 815–848.

Hartell, N.A. (1996). Strong activation of parallel fibers produces localized calcium transients and a form of LTD that spreads to distant synapses. Neuron *16*, 601–610.

Hartell, N.A. (2002). Parallel fiber plasticity. Cerebellum *1*, 3–18.

Hernjak, N., Slepchenko, B.M., Fernald, K., Fink, C.C., Fortin, D., Moraru, I.I., Watras, J., and Loew, L.M. (2005). Modeling and analysis of calcium signaling events leading to long-term depression in cerebellar Purkinje cells. Biophys. J. *89*, 3790–3806.

Ito, M. (2001). Cerebellar long-term depression: characterization, signal transduction, and functional roles. Physiol. Rev. *81*, 1143–1195.

Ito, M., and Kano, M. (1982). Long-lasting depression of parallel fiber-Purkinje cell transmission induced by conjunctive stimulation of parallel fibers and climbing fibers in the cerebellar cortex. Neurosci. Lett. *33*, 253–258.

Karachot, L., Kado, R.T., and Ito, M. (1994). Stimulus parameters for induction of long-term depression in in vitro rat Purkinje cells. Neurosci. Res. *21*, 161–168.

Kasono, K., and Hirano, T. (1994). Critical role of postsynaptic calcium in cerebellar long-term depression. Neuroreport *6*, 17–20.

Knight, B.W. (1972). Dynamics of encoding in a population of neurons. J. Gen. Physiol. *59*, 734–766.

Köhler, T., Heinisch, M., Kirchner, M., Peinhardt, G., Hirschelmann, R., and Nuhn, P. (1992). Phospholipase A_2 inhibition by alkylbenzoylacrylic acids. Biochem. Pharmacol. *44*, 805–813.

Konnerth, A., Dreessen, J., and Augustine, G.J. (1992). Brief dendritic calcium signals initiate long-lasting synaptic depression in cerebellar Purkinje cells. Proc. Natl. Acad. Sci. USA *89*, 7051–7055.

Kuroda, S., Schweighofer, N., and Kawato, M. (2001). Exploration of signal transduction pathways in cerebellar long-term depression by kinetic simulation. J. Neurosci. *21*, 5693–5702.

Launey, T., Endo, S., Sakai, R., Harano, J., and Ito, M. (2004). Protein phosphatase 2A inhibition induces cerebellar long-term depression and declustering of synaptic AMPA receptor. Proc. Natl. Acad. Sci. USA *101*, 676–681.

Lev-Ram, V., Jiang, T., Wood, J., Lawrence, D.S., and Tsien, R.Y. (1997). Synergies and coincidence requirements between NO, cGMP, and Ca^{2+} in the induction of cerebellar long-term depression. Neuron *18*, 1025–1038.

Lev-Ram, V., Wong, S.T., Storm, D.R., and Tsien, R.Y. (2002). A new form of cerebellar long-term potentiation is postsynaptic and depends on nitric oxide but not cAMP. Proc. Natl. Acad. Sci. USA *99*, 8389–8393.

Linden, D.J. (1994). Long-term synaptic depression in the mammalian brain. Neuron *12*, 457–472.

Linden, D.J. (1996). A protein synthesis-dependent late phase of cerebellar long-term depression. Neuron *17*, 483–490.

Linden, D.J., Dickinson, M.H., Smeyne, M., and Connor, J.A. (1991). A long-term depression of AMPA currents in cultured cerebellar Purkinje neurons. Neuron *7*, 81–89.

Lisman, J. (1989). A mechanism for the Hebb and the anti-Hebb processes underlying learning and memory. Proc. Natl. Acad. Sci. USA *86*, 9574–9578.

Maeda, H., Ellis-Davies, G.C., Ito, K., Miyashita, Y., and Kasai, H. (1999). Supralinear Ca^{2+} signaling by cooperative and mobile Ca^{2+} buffering in Purkinje neurons. Neuron *24*, 989–1002.

Malenka, R.C., and Bear, M.F. (2004). LTP and LTD: an embarrassment of riches. Neuron *44*, 5–21.

Marcaggi, P., Billups, D., and Attwell, D. (2003). The role of glial glutamate transporters in maintaining the independent operation of juvenile mouse cerebellar parallel fibre synapses. J. Physiol. *552*, 89–107.

Matsuda, S., Launey, T., Mikawa, S., and Hirai, H. (2000). Disruption of AMPA receptor GluR2 clusters following long-term depression induction in cerebellar Purkinje neurons. EMBO J. *19*, 2765–2774.

Miyakawa, H., Lev-Ram, V., Lasser-Ross, N., and Ross, W.N. (1992). Calcium transients evoked by climbing fiber and parallel fiber synaptic inputs in guinea pig cerebellar Purkinje neurons. J. Neurophysiol. *68*, 1178–1189.

Miyata, M., Finch, E.A., Khiroug, L., Hashimoto, K., Hayasaka, S., Oda, S.I., Inouye, M., Takagishi, Y., Augustine, G.J., and Kano, M. (2000).

Local calcium release in dendritic spines required for long-term synaptic depression. Neuron *28*, 233–244.

Morgan, J.R., Prasad, K., Hao, W., Augustine, G.J., and Lafer, E.M. (2000). A conserved clathrin assembly motif essential for synaptic vesicle endocytosis. J. Neurosci. *20*, 8667–8676.

Namiki, S., Kakizawa, S., Hirose, K., and Iino, M. (2005). NO signalling decodes frequency of neuronal activity and generates synapse-specific plasticity in mouse cerebellum. J. Physiol. *566*, 849–863.

Neveu, D., and Zucker, R.S. (1996). Postsynaptic levels of $[Ca^{2+}]_i$ needed to trigger LTD and LTP. Neuron *16*, 619–629.

Nevian, T., and Sakmann, B. (2006). Spine Ca^{2+} signaling in spike-timing-dependent plasticity. J. Neurosci. *26*, 11001–11013.

Oancea, E., and Meyer, T. (1998). Protein kinase C as a molecular machine for decoding calcium and diacylglycerol signals. Cell *95*, 307–318.

Ogasawara, H., Doi, T., Doya, K., and Kawato, M. (2007). Nitric oxide regulates input specificity of long-term depression and context dependence of cerebellar learning. PLoS Comput. Biol. *3*, e179. 10.1371/journal.pcbi.0020179.

Petersen, C.C., Malenka, R.C., Nicoll, R.A., and Hopfield, J.J. (1998). All-or-none potentiation at CA3-CA1 synapses. Proc. Natl. Acad. Sci. USA *95*, 4732–4737.

Reynolds, T., and Hartell, N.A. (2000). An evaluation of the synapse specificity of long-term depression induced in rat cerebellar slices. J. Physiol. *527*, 563–577.

Reynolds, T., and Hartell, N.A. (2001). Roles for nitric oxide and arachidonic acid in the induction of heterosynaptic cerebellar LTD. Neuroreport *12*, 133–136.

Ross, W.N., and Werman, R. (1987). Mapping calcium transients in the dendrites of Purkinje cells from the guinea-pig cerebellum in vitro. J. Physiol. *389*, 319–336.

Sakurai, M. (1990). Calcium is an intracellular mediator of the climbing fiber in induction of cerebellar long-term depression. Proc. Natl. Acad. Sci. USA *87*, 3383–3385.

Santamaria, F., Wils, S., De Schutter, E., and Augustine, G.J. (2006). Anomalous diffusion in dendrites caused by dendritic spines. Neuron *52*, 635–648.

Schmidt, H., Stiefel, K.M., Racay, P., Schwaller, B., and Eilers, J. (2003). Mutational analysis of dendritic Ca^{2+} kinetics in rodent Purkinje cells: role of parvalbumin and calbindin D28k. J. Physiol. *551*, 13–32.

Sepúlveda, M.R., Hidalgo-Sánchez, M., and Mata, A.M. (2004). Localization of endoplasmic reticulum and plasma membrane Ca^{2+}-ATPases in subcellular fractions and sections of pig cerebellum. Eur. J. Neurosci. *19*, 542–551.

Shenolikar, S. (1986). Control of cell function by reversible protein phosphorylation. J. Cyclic Nucleotide Protein Phosphor. Res. *11*, 531–541.

Shibuki, K., and Okada, D. (1992). Cerebellar long-term potentiation under suppressed postsynaptic Ca^{2+} activity. Neuroreport *3*, 231–234.

Sutton, R.B., and Sprang, S.R. (1998). Structure of the protein kinase Cbeta phospholipid-binding C2 domain complexed with Ca^{2+}. Structure *6*, 1395–1405.

Swandulla, D., Hans, M., Zipser, K., and Augustine, G.J. (1991). Role of residual calcium in synaptic depression and posttetanic potentiation: fast and slow calcium signaling in nerve terminals. Neuron *7*, 915–926.

Verdaguer, N., Corbalán-García, S., Ochoa, W.F., Fita, I., and Goméz-Fernandéz, J.C. (1999). Ca^{2+} bridges the C2 membrane-binding domain of protein kinase Calpha directly to phosphatidylserine. EMBO J. *18*, 6329–6338.

Wang, S.S., and Augustine, G.J. (1995). Confocal imaging and local photolysis of caged compounds: dual probes of synaptic function. Neuron *15*, 755–760.

Wang, Y.T., and Linden, D.J. (2000). Expression of cerebellar long-term depression requires postsynaptic clathrin-mediated endocytosis. Neuron *25*, 635–647.

Wang, S.S., Denk, W., and Häusser, M. (2000a). Coincidence detection in single dendritic spines mediated by calcium release. Nat. Neurosci. *3*, 1266–1273.

Wang, S.S., Khiroug, L., and Augustine, G.J. (2000b). Quantification of spread of cerebellar long-term depression with chemical two-photon uncaging of glutamate. Proc. Natl. Acad. Sci. USA *97*, 8635–8640.

Yang, S.N., Tang, Y.G., and Zucker, R.S. (1999). Selective induction of LTP and LTD by postsynaptic $[Ca^{2+}]_i$ elevation. J. Neurophysiol. *81*, 781–787.